Journal of Manufacturing Processes 31 (2018) 72–79

Contents lists available at ScienceDirect

Journal of Manufacturing Processes

journal homepage: www.elsevier.com/locate/manpro

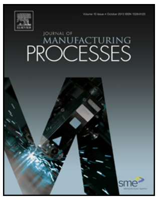

Research Paper

Numerical study of spatter formation during fiber laser welding of aluminum alloy

Dabin Zhang[a], Canli Li[b], Xixia Liu[a], Yang Cao[a], Dongsheng Wu[c,*]

[a] School of Mechanical Engineering, Guizhou University, Guiyang, Guizhou 550025, PR China
[b] Engineering Training Center, Guizhou University, Guiyang, Guizhou 550025, PR China
[c] Shanghai Power Equipment Research Institute, Shanghai 200240, PR China

ARTICLE INFO

Article history:
Received 18 June 2017
Received in revised form 29 October 2017
Accepted 3 November 2017

Keywords:
Laser welding
Aluminum alloy
Keyhole behavior
Spatter formation

ABSTRACT

The weld convection and spatter formation in aluminum alloy fiber laser welding are investigated based on numerical simulation and high speed photography results. It is found that a clockwise flow pattern exists in the rear part of the keyhole. The molten metal at the top surface of the rear part flows to the edge of the weld pool, owing to the surface tension gradient. The spatters generate mainly around the keyhole. The spatter formation sequence is that the formation of the swelling around the keyhole caused by the upward flowing molten metal, the increasing of the swelling size caused by the accumulation of vertical momentum, and the spatter ejection from the keyhole when the momentum of the molten metal is sufficient to overcome the surface tension. The recoil pressure caused by evaporation and the shear stress caused by metallic vapor flow are responsible for the spatter formation.

1. Introduction

Due to its excellent resistance to corrosion, weldability and formability, 5083 aluminum alloy is widely used in modern high speed train, liquefied natural gas (LNG) carrier and shipbuilding manufacturing industry. It is inevitable to join 5083 aluminum alloy by various welding methods, such as laser welding, owing to its low heat input and high depth to width ratio. During the laser welding, a deep keyhole is formed [1]. The spatter is generated when the momentum of a local volume of molten metal is high enough to overcome the surface tension force. The formation of spatter can also lead to other defects, such as underfilling and undercutting [2]. It has certain significance to study the formation mechanism of spatter in laser welding of 5083 aluminum alloy, and propose reasonable methods to reduce them.

Semak suggested that the recoil pressure caused the high-velocity-melt-flow ejection from the laser-metal interaction zone [3]. Fabbro proposed that the drag force caused by vapor could accelerate the molten metal around the keyhole, and leaded to droplet formation [4]. Kawahito proposed that the strong shear force of laser induced plume rather than recoil pressure was responsible for the formation of spatter [5]. Weberpals investigated the spatter formation based on high speed photographs, and found that the maximum ejection angle of droplets emitted from the rear part of the keyhole rim had linear relationship with keyhole front wall inclination [6]. Kaplan developed a systematic description of various types of spatter phenomenon in laser welding, and proposed a categorization system to facilitate the comparison and combination of research findings on spatter [7]. Zhang used a modified "sandwish" specimen to observe the geometry of the keyhole wall, he proposed that the recoil momentum associated with the energized vapor plume jet were responsible for the formation of high speed micro-spatter [8], with the use of bottom shielding gas, stable welding process and sound weld appearances at both the top and bottom surfaces can be obtained, when deep penetration laser welding of thick stainless steel with a 10 kw fiber laser [9]. Li used the high speed video cameras to observe the weld pool of glass and steel behind the keyhole, he proposed that the breaking of vapor generated wave was the key to explain the generation mechanism of swelling and spatter in high power deep penetration laser welding [10]. He also used a X-ray transmission imaging system to investigate the weld pool convection in the laser welding, and found that the behavior of the weld pool was the key factor to determine the spatter formation [11].

Currently, the spatter formation is studied mainly through experimental method and there is lack of modeling investigation due to its high complexity. Hugger used the commercial software OpenFOAM to model the detachment of droplets in laser welding,

---

* Corresponding author.
E-mail address: ctrj5xdmWDS@sina.com (D. Wu).

https://doi.org/10.1016/j.jmapro.2017.11.006
1526-6125/

Table 1
Thermo-physical material properties of 5083 aluminum alloy.

Nomenclature	Value	Nomenclature	Value
Density (l)	2380 (Kg/m^3)	Thermal conductivity (s)	235 (W/m K)
Density (s)	2660 (Kg/m^3)	Liquidus temperature	933 (K)
Viscosity	4.2×10^{-3} (Kg/m s)	Solidus temperature	847 (K)
Specific heat (l)	1197.21 (J/kg K)	Boiling temperature	2720 (K)
Specific heat (s)	1050 (J/kg K)	Heat transfer coefficient	20 (W/m^2 K^4)
Latent heat of fusion	3.87×10^5 (J/kg)	Coefficient of thermal expansion	1.5×10^{-4} (K^{-1})
Latent heat of vapor	1.05×10^7 (J/kg)	Surface tension	0.871 (N/m)
Thermal conductivity (l)	90 (W/m K)	Surface tension gradient	-0.000155 (N/m K)

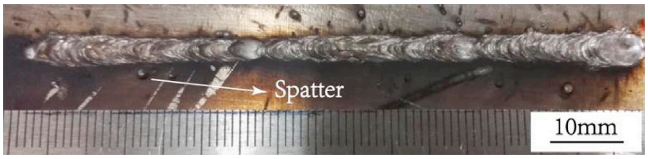

Fig. 1. Weld seam appearances of 5083 aluminum alloy (laser power 5 kw, welding speed 2 m/min).

but the behavior of the weld pool had not been discussed [12]. Chang built a CFD model to analyze the formation mechanism of spatter, and found that the occurrence of spatter was closely related to the flow velocity and vorticity in the weld pool, however the effect ofkeyhole was ignored in the model [13].

In this article, a three-dimensional numerical model is established to investigate the spatter formation in fiber laser welding of 5083 aluminum alloy, the shear stress caused by the metallic vapor flow is considered, the fluid flow features within the weld pool and the formation mechanism of spatter are discussed.

2. Experimental procedure

A fiber laser welding machine (IPG YLS-10000) with output wavelength 1070 ± 10 nm, focus radius 0.36 mm, is used in the welding experiments, the laser power is 5 kw, the defocused distance is 0 mm, the welding speed is 2 m/min, pure argon gas is used as shielding gas with a flow rate of 20 L/min, the nozzle is placed at the trailing position with a typical inclination of 45° . The material used is 10 mm-thick 5083 aluminum alloy, the thermo-physical material properties of the base metal is shown in Table 1. The top views of the weld beads are displayed in Fig. 1 . A high speed video camera is used to observe the weld pool behavior and spatter formation, a band pass filter with a transmission band of 808 nm is positioned in front of the camera lens to filter out unwanted light, the frequency is 5000 frame/s, a diode laser (λ = 806 ± 10 nm) with a maximum power of 300 W is used to illuminate the welding zone.

3. Mathematical model and numerical simulation

3.1. Governing equations

The governing equations for laser welding simulation are mass, momentum, energy equations, and the VOF (Volume of Fluid) [14]. The flow inside the weld pool is laminar, the liquid metal is considered to be a Newtonian and incompressible fluid, the effects of shielding gas and Knudsen layer near the keyhole are omitted.

Mass conservation equation:

$$\nabla \cdot \vec{V} = 0 \tag{1}$$

Navier-Stokes equation:

$$\frac{\partial \vec{V}}{\partial t} + \vec{V} \cdot \nabla \vec{V} = -\frac{1}{\rho} \nabla P + \mu \nabla^2 \vec{V} - K\vec{V} + \mathrm{f} \tag{2}$$

Energy conservation equation:

$$\rho \left(\frac{\partial h}{\partial t} + \vec{V} \cdot \nabla h \right) = \nabla \cdot (\kappa \nabla T) \tag{3}$$

VOF equation:

$$\frac{\partial F}{\partial t} + \nabla \left(\vec{V}.F \right) = 0 \tag{4}$$

The following enthalpy based continuum model is used to model the solid-liquid phase change.

$$h = \begin{cases} \rho_s C_s T & (T \le T_s) \\ h(T_s) + h_{sl} \dfrac{T - T_s}{T_l - T_s} & (T_s < T \le T_l) \\ h(T_l) + \rho_l C_l (T - T_l) & (T_l < T) \end{cases} \tag{5}$$

The porous media drag model is used to model the flow in the mushy zone in which the temperature of the cell is between liquidus and solidus temperature.The drag coefficient is:

$$K = \frac{C{F_s}^2}{(1 - F_s)^3} \tag{6}$$

3.2. Driven forces

A simple recoil force model derived from the Clausius-Clapeyron equation is used [15]:

$$\mathrm{P_r} = 0.54 P_0 \exp \left(L_v \frac{T - T_b}{\bar{R} T T_b} \right) \tag{7}$$

The buoyancy force inside the weld pool can be expressed as follow:

$$F_b = \rho g \beta (T - T_0) \tag{8}$$

The surface tension of the liquid metal can be expressed as a linear function of temperature:

$$\gamma = \gamma_0 + \frac{d\gamma}{dT}(T - T_0) \tag{9}$$

The shear stress caused by metallic vapor flow is considered [16]:

$$\tau_w = \frac{8 \rho V^2}{Re} \tag{10}$$

V is the vapor velocity, it is assumed that the vapor velocity increases linearly from keyhole bottom to the entrance of the keyhole. In this study, the average vapor velocity at the entrance of the keyhole is 150 m/s.